SAKARYA ÜNİVERSİTESİ
FEN BİLİMLERİ ENSTİTÜSÜ DERGİSİ

Sakarya University Journal of Science
SAUJS

e-ISSN 2147-835X | Period Bimonthly | Founded: 1997 | Publisher Sakarya University |
http://www.saujs.sakarya.edu.tr/en/

Title: Process Model Development of Lithium-ion Batteries — An Electrochemical Impedance Spectroscopy Simulation

Authors: Salim EROL
Recieved: 2020-07-07 12:16:16

Accepted: 2020-09-08 15:38:37

Article Type: Research Article

Volume: 24
Issue: 6
Month: December
Year: 2020
Pages: 1191-1197

How to cite
Salim EROL; (2020), Process Model Development of Lithium-ion Batteries — An Electrochemical Impedance Spectroscopy Simulation. Sakarya University Journal of Science, 24(6), 1191-1197, DOI: https://doi.org/10.16984/saufenbilder.765554
Access link
http://www.saujs.sakarya.edu.tr/en/pub/issue/57766/765554

Sakarya University Journal of Science 24(6), 1191-1197, 2020

Process Model Development of Lithium-ion Batteries — An Electrochemical Impedance Spectroscopy Simulation

Salim EROL*[1]

Abstract

In this study, a simulation of an electrochemical impedance spectroscopy for lithium-ion batteries was proposed. The electrochemical process was developed from battery electrode kinetics and mass transfer of mobile Li^+ ions through negative and positive electrodes and electrolyte. The phenomena used in this process were represented by an equivalent electrical circuit. A mathematical model was designed using the equivalent circuit and its elements which are in fact battery parameters. The parameter values were presented as compared with real experimental impedance result. The results showed that the simulation and process development were in good agreement with the experimental data.

Keywords: Li-ion battery, impedance spectroscopy, equivalent electrical circuit, porous electrode, solid electrolyte interphase

1. INTRODUCTION

Electrochemical impedance spectroscopy (EIS) is a broadly used noninvasive technique for variety of systems including batteries [1-5], fuel cells [6-9], corrosion detecting [10-14], biosensors [15-19], and so on [20].

Typical representation of EIS of an electrochemical system is complex Nyquist diagram. The Nyquist plot a Li-ion battery shown in Figure 1 can be divided into two regions of high frequency and low frequency. The high frequency region is between points corresponding to 100 kHz and 0.5 Hz. The low frequency region is between points corresponding to 0.5 Hz and 20 mHz. Initial examination of the Nyquist plot the following points can be attested as:

1. The high frequency zone corresponds to the interfacial charge transfer kinetics on electrodes.

2. The low frequency zone corresponds that of a diffusion process in a solid phase.

* Corresponding Author: esalim@ogu.edu.tr
[1] Eskişehir Osmangazi University, ORCID: https://orcid.org/0000-0002-7219-6642

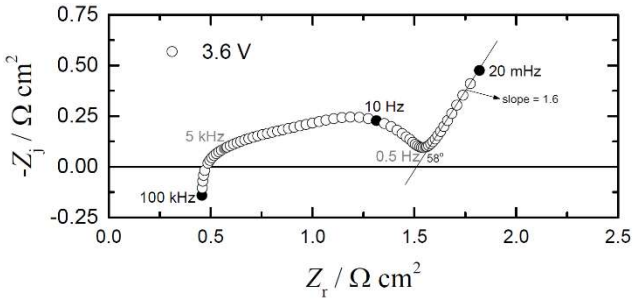

Figure 1 Typical impedance response of a Li-ion battery at 3.6 V cell potential [21]

The objective of the study is to represent a new simulation approach along with a realistic process development for an EIS of the Li-ion batteries.

2. PROCESS DEVELOPMENT

Two prominent theories explain the process of a Li-ion battery. The theory by Doyle et al. [22,23], describes the battery process as given in Figure 1. The battery is considered to include a porous negative electrode, a separator, and a porous positive electrode. Li^+ ions from the positive electrode are released, travel through the electrolyte in the separator region, and are then intercalated into the negative electrode. The following processes may be considered to take place:

1. The de-intercalation reaction of the Li^+ ions in the porous positive electrode.
2. The diffusion of Li^+ ions in the solid phase of positive electrode.
3. Transport of solution in the porous electrode in the positive electrode.
4. Transport of Li^+ ions through the electrolyte in separator region.
5. Transport of solution in porous electrode in the negative electrode.
6. Diffusion of Li^+ ions in the solid phase in the negative electrode.
7. Intercalation reaction of the Li^+ ions in the porous negative electrode.

Along with the above processes, charging of the double layer takes place at both the electrodes. In the analysis charging and Faradaic currents are assumed to be separable, side reactions at the electrode-electrolyte interface are neglected, and Butler-Volmer kinetics are assumed to apply for the reactions at both electrodes. For a single reversible electrochemical reaction, the Butler-Volmer equation is expressed as

$$i = i_0 \left\{ \exp\left[\frac{(1-\alpha)n\mathrm{F}}{\mathrm{R}T}\eta_s\right] - \exp\left(-\frac{\alpha n\mathrm{F}}{\mathrm{R}T}\eta_s\right)\right\} \quad (1)$$

where i is the current density, i_0 is called the exchange current density which is the current at zero surface overpotential, η_s is the surface overpotential representing the departure from an equilibrium potential, α is called symmetry factor which is the fraction of the surface overpotential that is with respect to the cathodic reaction, n is the number of electrons transferred through the electrodes, F is the Faraday's constant, R is the universal gas constant, and T is absolute temperature [24].

Doyle et al. [22,23] used a set of equations for the above process and, solving those equations with specific set of conditions, established various parameter relations which enabled them to simulate the impedance spectra and compare it with those of experimental spectra. The complete analysis of the impedance spectra by Doyle et al. enabled them to distinguish the various factors of the battery by separating the terms of the equations which symbolized different processes of the battery. The analysis revealed that the high frequency region of the impedance spectra was mainly due to the interfacial kinetic resistance contributed primarily by the intercalation reaction. It also depended on the depth of discharge of the Li^+ ions. The charge transfer resistance of the de-intercalation reaction is a primary contributor when the depth of discharge was >80% or <20%. The low-frequency region was attributed to the diffusion impedance in the solution phase and the solid phase and to the capacitive double layers at the interface. The summation of all the above regions gave impedance spectra similar to that of the low frequency region.

The other theory, as represented by Aurbach [25], considers a different lithiated graphite electrode structure. This theory places more importance to the reactions at the electrode–electrolyte interface. These reactions lead to the development of an additional film at the interface called the solid electrolyte interphase (SEI). This film also

explains the rise in impedance response on cycling of the cell due to continuous formation of additional film during the operation of the battery. The model envisions transport of Li^+ ions through different phases of the film and the final assimilation of Li^+ ions in the negative electrode. Unlike the process described by Doyle et al., interfacial kinetics in the porous electrode is not considered. Instead, diffusion of the Li^+ ions is assumed to occur in the electrode until they reach their final destination. This leads to development of capacitance inside the electrode. Also films on the surface provide different phases; hence, they too contribute to capacitance.

3. MATHEMATICAL MODEL

According to the model that was developed considering the two theories described above, the stages of the battery process are assumed to include:

1. The formation of an SEI due to Li^+ ions reductive strength on the electrode surface,
2. The de-intercalation of Li^+ ions from the positive electrode,
3. Diffusion of Li^+ ions in the solid phase,
4. Transport of solution through the porous electrode and then across the SEI, and
5. Diffusion of Li^+ ions through the electrolyte in the separator.

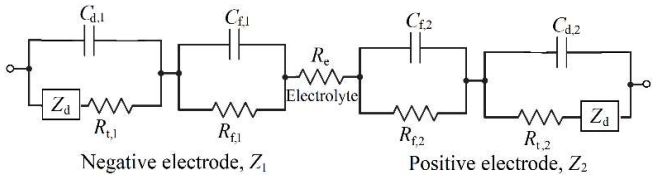

Figure 2 Proposed equivalent electrical circuit for EIS of Li-ion battery

Similar processes are added from stage 1 to 5 in reverse order across the negative electrode with de-intercalation replaced by intercalation reaction in the negative electrode. The capacitance is assumed to exist at both the SEI and the double layer at the electrode surface. The corresponding equivalent circuit is presented as Figure 2.

The impedance of the above circuit can be expressed as

$$Z = Z_1 + R_e + Z_2 \tag{2}$$

where R_e is the ohmic resistance or the electrolyte resistance; Z_1 and Z_2 are the impedances of corresponding to the negative and positive electrodes, respectively. They are expressed as:

$$Z_1 = \frac{R_{t,1}+Z_d}{1+j\omega(R_{t,1}+Z_d)C_{d,1}} + \frac{R_{f,1}}{1+j\omega R_{f,1}C_{f,1}} \tag{3}$$

and

$$Z_2 = \frac{R_{f,2}}{1+j\omega R_{f,2}C_{f,2}} + \frac{R_{t,2}+Z_d}{1+j\omega(R_{t,2}+Z_d)C_{d,2}} \tag{4}$$

where R_f refers to the SEI film resistances, R_t refers to the charge transfer resistances for the electrode reactions which are intercalation and de-intercalation processes, C_f refers to capacitance representing SEI layer, C_d is the double layer capacitance on the electrode surfaces, and Z_d is the diffusion impedance occurring in both negative and positive electrodes and expressed as:

$$Z_d(\omega) = Z_d(0)\frac{\coth(\sqrt{jK})}{\sqrt{jK}} \tag{5}$$

where $Z_d(0)$ refers to the diffusion impedance corresponding to the zero frequency ($f = 0$), and K is the dimensionless frequency given as:

$$K = \frac{\omega\delta^2}{D_{Li^+}} \tag{6}$$

where δ is the Li^+ ion diffusion layer thickness, and D_{Li^+} is the diffusivity of Li^+ ions. In above Equations (2-6), ω is the angular frequency which is equal to $2\pi f$, and j refers to the imaginary number which is expressed as $j^2 = -1$.

4. RESULTS AND DISCUSSION

A typical impedance simulation is presented in Figure 3 using the frequency range between 10 kHz to 10 mHz. The model parameters used to obtain this result are presented in Table 1.

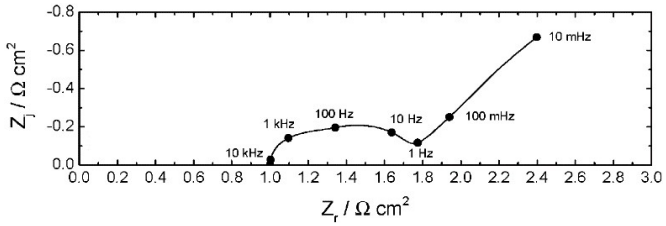

Figure 3 Simulation result for the impedance model in Equations (2-6) shown with the line. The corresponding frequencies are indicated with dots

A certain amount of positive imaginary impedance (Z_j) values can be observed in Figure 1 at a typical impedance response of the Li-ion battery. That type of response is generally interpreted to an inductive behavior of the electrochemical system interested in. However, it is not a case for an energy storage device such as batteries. This inductive behavior at very high frequencies is attributed to noise or impedance related to connection cables in the experimental setup of the Li-ion battery cell. Therefore, only negative values of imaginary impedance forming capacitive loop at high frequencies are observed in the simulation shown in Figure. While doing regression on impedance data, like applied in recently published publications [26-30], one should keep in mind that the positive values of Z_j could be truncated. Thus, no inductive loop could be observed in the simulation result in Figure 3. Also, there are three capacitive loops combined in the simulation constituting a compressed circle like shape similar to the experimental data shown in Figure 1. The large capacitance values in Table 1 forming the capacitive loops here are consistent with assumption of a porous electrode. The capacitive loops are corresponding to the negative electrode, the SEI layer, and the positive electrode. The interception the line of this loop with real impedance (Z_r) axis represents the electrolyte resistance (R_e). If the line is extrapolated to Z_r axis at lower frequencies at the high frequency region, e.g. 10 Hz in Figure 3, the value here is equal to sum of all resistances in the equivalent circuit that are R_e, $R_{f,1}$, $R_{t,1}$, $R_{f,2}$, and $R_{t,2}$. The straight line at low frequencies is attributed to diffusion impedance (Z_d). The simulation values of all above mentioned parameters are indicated in Table 1. The values were selected from the nonrealistic point of view. The aim is to find similar impedance results for Li-ion batteries as obtained in EIS experiments.

Table 1
Model parameters used for the simulation result presented in Figure 3

Parameter	Value
R_e	1.0 Ωcm^2
$R_{f,1}$	0.15 Ωcm^2
$R_{f,2}$	0.15 Ωcm^2
$R_{t,1}$	0.20 Ωcm^2
$R_{t,2}$	0.20 Ωcm^2
$C_{f,1}$	3.16×10^{-3} F/cm^2
$C_{f,2}$	1.00×10^{-2} F/cm^2
$C_{d,1}$	3.16×10^{-2} F/cm^2
$C_{d,2}$	1.00×10^{-1} F/cm^2
D_{Li^+}	1.5×10^{-10} m^2/s
δ	1.5×10^{-4} m
$Z_d(0)$	1.5 Ωcm^2

5. CONCLUSIONS

A detailed preliminary Li-ion battery process model and its mathematical representation in terms of impedance spectroscopy were proposed in this study. Obtained parameters from the equivalent circuit initiate and boost electrochemical modeling for rechargeable batteries. An example of impedance simulation for a Li-ion battery was presented as a result here to express an equivalent circuit of passive electrical elements each representing a physical process. The results show that simulation model could be utilized for modeling Li-ion batteries. This study will give guidance for simulating and modeling not only batteries but also other types of energy storage devices.

Funding

The author received no financial support for the research, authorship, and/or publication of this paper.

The Declaration of Conflict of Interest/ Common Interest

No conflict of interest or common interest has been declared by the author.

The Declaration of Ethics Committee Approval

The author declares that this document does not require an ethics committee approval or any special permission.

The Declaration of Research and Publication Ethics

The author of the paper declares that he complies with the scientific, ethical and quotation rules of SAUJS in all processes of the paper and that he does not make any falsification on the data collected. In addition, he declares that Sakarya University Journal of Science and its editorial board have no responsibility for any ethical violations that may be encountered, and that this study has not been evaluated in any academic publication environment other than Sakarya University Journal of Science.

REFERENCES

[1] S. Buller, M. Thele, E. Karden, and R. W. De Doncker, "Impedance-based non-linear dynamic battery modeling for automotive applications," Journal of Power Sources, vol. 113, no. 2, pp. 422-430, 2003.

[2] H. Blanke et al., "Impedance measurements on lead–acid batteries for state-of-charge, state-of-health and cranking capability prognosis in electric and hybrid electric vehicles," Journal of power Sources, vol. 144, no. 2, pp. 418-425, 2005.

[3] W. Waag, S. Käbitz, and D. U. Sauer, "Experimental investigation of the lithium-ion battery impedance characteristic at various conditions and aging states and its influence on the application," Applied energy, vol. 102, pp. 885-897, 2013.

[4] W. Huang and J. A. A. Qahouq, "An online battery impedance measurement method using DC–DC power converter control," IEEE Transactions on Industrial Electronics, vol. 61, no. 11, pp. 5987-5995, 2014.

[5] J. Landesfeind, D. Pritzl, and H. A. Gasteiger, "An analysis protocol for three-electrode li-ion battery impedance spectra: Part i. analysis of a high-voltage positive electrode," Journal of The Electrochemical Society, vol. 164, no. 7, p. A1773, 2017.

[6] Z. He and F. Mansfeld, "Exploring the use of electrochemical impedance spectroscopy (EIS) in microbial fuel cell studies," Energy & Environmental Science, vol. 2, no. 2, pp. 215-219, 2009.

[7] J. T. Müller, P. M. Urban, and W. F. Hölderich, "Impedance studies on direct methanol fuel cell anodes," Journal of Power Sources, vol. 84, no. 2, pp. 157-160, 1999.

[8] N. Fouquet, C. Doulet, C. Nouillant, G. Dauphin-Tanguy, and B. Ould-Bouamama, "Model based PEM fuel cell state-of-health monitoring via ac impedance measurements," Journal of Power Sources, vol. 159, no. 2, pp. 905-913, 2006.

[9] A. Weiß, S. Schindler, S. Galbiati, M. A. Danzer, and R. Zeis, "Distribution of relaxation times analysis of high-temperature PEM fuel cell impedance spectra," Electrochimica Acta, vol. 230, pp. 391-398, 2017.

[10] M. Kendig, F. Mansfeld, and S. Tsai, "Determination of the long term corrosion behavior of coated steel with AC impedance measurements," Corrosion Science, vol. 23, no. 4, pp. 317-329, 1983.

[11] J. Zhang, P. J. Monteiro, and H. F. Morrison, "Noninvasive surface measurement of corrosion impedance of reinforcing bar in concrete—part 1: experimental results," Materials Journal, vol. 98, no. 2, pp. 116-125, 2001.

[12] K. Jüttner and W. Lorenz, "Electrochemical impedance spectroscopy (EIS) of corrosion processes on inhomogeneous surfaces," in Materials Science Forum, 1989, vol. 44, pp. 191-204: Trans Tech Publ.

[13] M. Behzadnasab, S. Mirabedini, M. Esfandeh, and R. Farnood, "Evaluation of

corrosion performance of a self-healing epoxy-based coating containing linseed oil-filled microcapsules via electrochemical impedance spectroscopy," Progress in Organic Coatings, vol. 105, pp. 212-224, 2017.

[14] J. C. Gomez-Vidal, A. Fernandez, R. Tirawat, C. Turchi, and W. Huddleston, "Corrosion resistance of alumina forming alloys against molten chlorides for energy production. II: Electrochemical impedance spectroscopy under thermal cycling conditions," Solar Energy Materials and Solar Cells, vol. 166, pp. 234-245, 2017.

[15] E. Katz and I. Willner, "Probing biomolecular interactions at conductive and semiconductive surfaces by impedance spectroscopy: routes to impedimetric immunosensors, DNA-sensors, and enzyme biosensors," Electroanalysis: An International Journal Devoted to Fundamental and Practical Aspects of Electroanalysis, vol. 15, no. 11, pp. 913-947, 2003.

[16] M. Varshney and Y. Li, "Interdigitated array microelectrodes based impedance biosensors for detection of bacterial cells," Biosensors and Bioelectronics, vol. 24, no. 10, pp. 2951-2960, 2009.

[17] A. Manickam, A. Chevalier, M. McDermott, A. D. Ellington, and A. Hassibi, "A CMOS electrochemical impedance spectroscopy (EIS) biosensor array," IEEE Transactions on Biomedical Circuits and Systems, vol. 4, no. 6, pp. 379-390, 2010.

[18] W. Cai, S. Xie, J. Zhang, D. Tang, and Y. Tang, "An electrochemical impedance biosensor for Hg2+ detection based on DNA hydrogel by coupling with DNAzyme-assisted target recycling and hybridization chain reaction," Biosensors and Bioelectronics, vol. 98, pp. 466-472, 2017.

[19] J. Dailey, M. Fichera, E. Silbergeld, and H. E. Katz, "Impedance spectroscopic detection of binding and reactions in acid-labile dielectric polymers for biosensor applications," Journal of Materials Chemistry B, vol. 6, no. 19, pp. 2972-2981, 2018.

[20] N. Bonanos et al., "Applications of impedance spectroscopy," Impedance spectroscopy: Theory, experiment, and applications, pp. 175-478, 2018.

[21] S. Erol, "Electrochemical impedance spectroscopy analysis and modeling of lithium cobalt oxide/carbon batteries," Ph.D. Dissertation, University of Florida, 2015.

[22] M. Doyle, J. P. Meyers, and J. Newman, "Computer simulations of the impedance response of lithium rechargeable batteries," Journal of the Electrochemical Society, vol. 147, no. 1, p. 99, 2000.

[23] M. Doyle and J. Newman, "Modeling the performance of rechargeable lithium-based cells: design correlations for limiting cases," Journal of Power Sources, vol. 54, no. 1, pp. 46-51, 1995.

[24] T. F. Fuller and J. N. Harb, Electrochemical engineering. John Wiley & Sons, 2018.

[25] D. Aurbach, "Review of selected electrode–solution interactions which determine the performance of Li and Li ion batteries," Journal of Power Sources, vol. 89, no. 2, pp. 206-218, 2000.

[26] U. Morali and S. Erol, "Analysis of electrochemical impedance spectroscopy response for commercial lithium-ion batteries: modeling of equivalent circuit elements," Turkish Journal of Chemistry, vol. 44, no. 3, pp. 602-613, 2020.

[27] U. Morali and S. Erol, "The comparison of electrochemical impedance behaviors of lithium-ion and nickel-metal hydride batteries at different state-of-charge conditions," Journal of the Engineering and Architecture Faculty of Eskişehir Osmangazi University, vol. 28, no. 1, pp. 1-8, 2020.

[28] U. Morali, "Influence of charge conditions on battery dynamics of a commercial lithium-ion cell," Hacettepe Journal of Biology and Chemistry, vol. 48, no. 3, pp. 203-210, 2020.

[29] U. Morali and S. Erol, "Electrochemical impedance analysis of 18650 lithium-ion and 6HR61 nickel-metal hydride rechargeable batteries," Journal of the Faculty of Engineering and Architecture of Gazi University, vol. 35, no. 1, pp. 297-310, 2020.

[30] S. Erol, Impedance Analysis and Modeling of Lithium-ion Batteries. Lap Lambert, 2016.